JMB

Unique Iron Binding and Oxidation Properties of Human Mitochondrial Ferritin: A Comparative Analysis with Human H-chain Ferritin

Fadi Bou-Abdallah[1]*, Paolo Santambrogio[2], Sonia Levi[2], Paolo Arosio[3] and N. Dennis Chasteen[1]*

[1]*Department of Chemistry University of New Hampshire Durham, NH 03824, USA*

[2]*DIBIT-San Raffaele Scientific Institute, Via Olgettina 58 20132 Milano, Italy*

[3]*Dipartimento Materno Infantile e Tecnologie Biomediche, Universita' di Brescia, A. O. Spedali Civili 25100 Brescia, Italy*

Ferritins are ubiquitous iron mineralizing and storage proteins that play an important role in iron homeostasis. Although excess iron is stored in the cytoplasm, most of the metabolically active iron is processed in the mitochondria of the cell. Little is known about how these organelles regulate iron homeostasis and toxicity. The recently discovered human mitochondrial ferritin (MtF), unlike other mammalian ferritins, is a homopolymer of 24 subunits that has a high degree of sequence homology with human H-chain ferritin (HuHF). Parallel experiments with MtF and HuHF reported here reveal striking differences in their iron oxidation and hydrolysis chemistry despite their similar diFe ferroxidase centers. In contrast to HuHF, MtF does not regenerate its ferroxidase activity after oxidation of its initial complement of Fe(II) and generally has considerably slower ferroxidation and mineralization activities as well. MtF exhibits sigmoidal kinetics of mineralization more characteristic of an L-chain than an H-chain ferritin. Site-directed mutagenesis reveals that serine 144, a residue situated near the ferroxidase center in MtF but absent from HuHF, is one player in this impairment of activity. Additionally only one-half of the 24 ferroxidase centers of MtF are functional, further contributing to its lower activity. Stopped-flow absorption spectrometry of Fe(II) oxidation by O_2 in MtF shows the formation of a transient diiron(III) μ-peroxo species ($\lambda_{max} = 650$ nm) as observed in HuHF. Also, as for HuHF, minimal hydroxyl radical is produced during the oxidative deposition of iron in MtF using O_2 as the oxidant. However, the $2Fe(II) + H_2O_2$ detoxification reaction found in HuHF does not occur in MtF. The structural differences and the physiological implications of the unique iron oxidation properties of MtF are discussed in light of these results.

© 2005 Elsevier Ltd. All rights reserved.

Keywords: mitochondria; ferritin; iron toxicity; oxidative stress; mineralization

*Corresponding authors

Abbreviations used: MtF, human mitochondrial ferritin; HuHF, human H-chain ferritin; MoHF, mouse H-chain ferritin; S144A, S144A/R60H, S144A/T63R and S144A/Y34F, human mitochondrial ferritin variants; Dps, DNA binding protein from starved cells; EMPO, 5-ethoxycarbonyl-5-methyl-1-pyrroline-*N*-oxide; EPR, electron paramagnetic resonance; Mops, 3-(*N*-morpholino) propane-sulfonic acid; Mes, (2-(*N*-morpholino) ethanesulfonic acid); Hepes, *N*-2-hydroxyethyl-piperazine-*N'*-2-ethanesulfonic acid.

E-mail addresses of the corresponding authors: fadib@cisunix.unh.edu; ndc@cisunix.unh.edu

Introduction

Iron is a vital element for almost all living organisms due to its essential role in numerous metabolic processes including oxygen transport, DNA synthesis, nitrogen fixation, electron transport, and photosynthesis.[1,2] Excess free iron has been implicated in neurodegenerative diseases, apoptosis, and also in the generation of harmful free radicals that cause damage to membranes, proteins and nucleic acids.[3,4] The low solubility of iron(III) at physiological conditions ($\sim 10^{-18}$ M) has compelled living organisms to adapt efficient iron transport and storage mechanisms. One for

overcoming iron toxicity and solubility is ferritin, a ubiquitous iron storage and biomineralizing protein found highly conserved in species from bacteria to plants to humans.[1,2,5,6] In bacteria and plants, ferritins are composed of 24 subunits of the same type, whereas in mammals they are of two types, H and L. Depending on the tissue type, the H and L subunits co-assemble in different ratios to form a protein shell of 24 subunits capable of acquiring ~ 4000 iron atoms per shell.[5] The H-chain subunit has ferroxidase activity associated with a di-iron binding center that is responsible for the rapid oxidation of Fe(II) to Fe(III) whereas the L-chain subunit appears to provide efficient sites for iron nucleation and mineralization.[5,7–10] In amphibian red cells, three types of subunits (M, H, and L) form heteropolymer ferritins.[2,5]

Each ferritin subunit, regardless of type (M, H or L), folds into four α-helix bundles (A, B, C, D) with a short fifth α-helix (E) at the C terminus and a loop connecting the helix pairs A–B and C–D. Although the amino acid sequence homology between ferritins from different species can be as low as 15%, their three-dimensional structures are remarkably conserved.[1,2,5] The 24 subunits assemble to form a nearly spherical structure of $4:3:2$ octahedral symmetry containing the mineralized iron core. The DNA binding protein from starved cells (Dps) class of iron binding proteins such as those from *Listeria innocua* and *Escherichia coli*[11,12] assemble to form a shell-like structure of 12 identical subunits related by $3:2$ tetrahedral symmetry and also contain an iron core. A recent study with the *E. coli* Dps showed a dual protective effect of the protein against DNA oxidative damage and the deleterious effect of Fe(II) and hydrogen peroxide.[13]

Reactive oxygen species (ROS) are continuously generated inside the mitochondria through the one electron reduction of oxygen during intermediate steps of the electron transport chain and have been implicated in cellular damage and aging-related diseases.[14] The free iron present inside the mitochondria may interact with these ROS to produce toxic hydroxyl radical through Fenton chemistry. Since the mitochondria are exposed to heavy trafficking of iron for the synthesis of heme and iron–sulfur clusters, they require an efficient mechanism to overcome the toxicity of iron. The recent discoveries of several new mitochondrial iron binding proteins have important implications for mitochondrial iron homeostasis.[15–20]

Most known ferritins are cytosolic proteins. However, a new type of ferritin has been recently identified as a homopolymer of 24 identical subunits that is located inside the matrix of human mitochondria and is encoded by an intronless gene on chromosome 5q23.1. It has a high degree of sequence homology (79%) with human H-chain ferritin (HuHF).[21,22] Here, we explore the structural and functional properties of this recently discovered mitochondrial ferritin and probe in detail its ferroxidase properties using spectroscopic and chemical methodologies. Unlike human H-ferritin (HuHF) where 48 Fe(II) bind and form dimeric Fe(III) species (two Fe^{3+} per ferroxidase center), mitochondrial ferritin (MtF) binds and oxidizes only 24 Fe(II), indicating that only half of the 24 ferroxidase centers of this protein are functional. The two proteins also differ markedly in their mineralization properties; HuHF displays hyperbolic kinetics of mineralization characteristic of a protein catalyzed reaction whereas the kinetics for MtF are sigmoidal as expected of an autocatalytic mineral surface mechanism similar to that seen with L-chain ferritin. The $(2Fe(II) + H_2O_2)$ detoxification reaction seen in HuHF[23] is absent in MtF. These major differences in the iron binding and oxidation properties suggest that MtF functions differently as an iron storage protein within the mitochondria and perhaps has other function(s) in iron homeostasis as well.

Results

Iron(III) binding stoichiometry

The amino acid residues constituting the ferroxidase centers of HuHF and MtF are conserved but, as shown below, the two proteins exhibit significantly different iron binding and oxidation properties. Here, we use UV–visible and fluorescence spectrophotometry, electrode oximetry, and pH-stat to study iron oxidation and binding in MtF and its variant S144A and compare the results to those of HuHF. Variant S144A is of interest because alanine 144, a residue in close proximity to the ferroxidase center in HuHF, is substituted by serine in MtF and Ser144 has been recently suggested to hinder the access of iron to the ferroxidase center of this protein.[24]

To measure the stoichiometry of Fe(III) binding to MtF, Fe(II) was presented to the apoprotein and allowed to oxidize to Fe(III) by di-oxygen. Figure 1(a) shows the absorbance changes at 350 nm upon multiple aerobic additions of five Fe(II)/MtF to the same MtF sample at pH 7.0. Surprisingly, and unlike other mammalian ferritins, where 48 Fe(III) bind (two at each of the 24 ferroxidase centers), a discontinuity in absorbance at ~ 24 Fe(III)/protein is obtained with both MtF (Figure 1(a)) and variant S144A (not shown). In accord with the UV result, quenching of the fluorescence intensity upon titration of the apoMtF with Fe(II) in the presence of molecular oxygen to produce Fe(III) also showed a stoichiometry of ~ 24 Fe(III) per protein (Figure 1(b)). Similarly, when Fe(II) was added to the same protein sample in increments of 7.5 Fe(II) per protein, the initial rates of iron oxidation and proton production, as measured separately by electrode oximetry and pH-stat, indicated the binding and oxidation of only 24 Fe(II) per protein (Figure 1(c)). Together, these data indicate that MtF and variant S144A bind only 24 Fe(III); either one site of each of the 24 dinuclear ferroxidase centers of these proteins is occupied by iron or only one out of
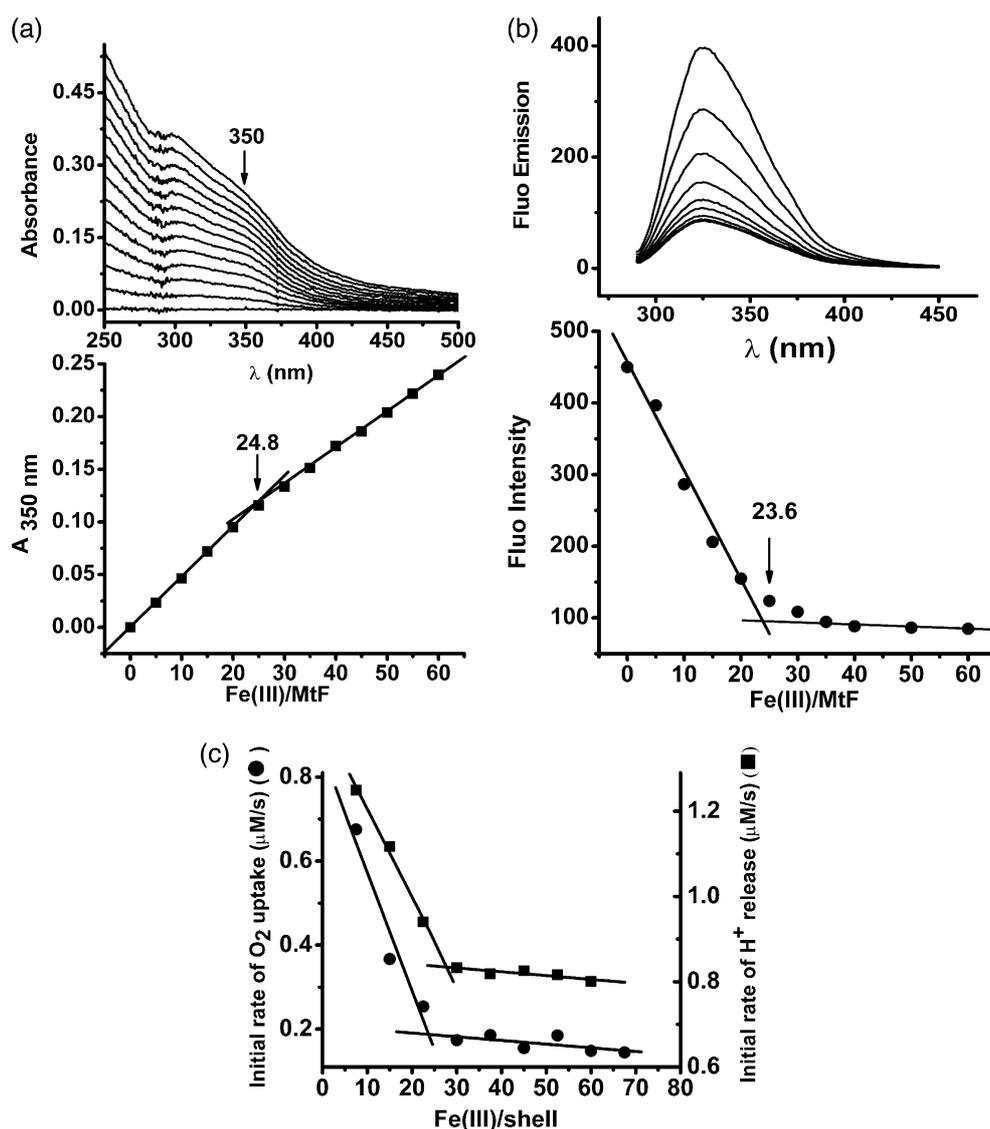
Figure 1. (a) Aerobic spectrophotometric and (b) fluorescence titration of MtF with Fe(II). Conditions: 2 μM protein, 10 μM Fe(II) (five Fe(II)/shell per injection), 50 mM Mops, and 50 mM NaCl for the absorbance data, 2.35 μM protein, 11.75 μM Fe(II) (five Fe(II)/shell per injection), and 100 mM Mops for the fluorescence data, pH 7.0 and 25 °C. (c) Initial rates of oxygen uptake and proton production as a function of Fe(II) loadings into MtF. Conditions: 2 μM protein, 15 μM Fe(II) (7.5 Fe(II)/shell per injection), 0.3 mM Mes, 100 mM NaCl, pH 6.51 controlled by the pH-stat, 25 °C.

two of the 24 ferroxidase centers binds iron. As shown below, the latter situation is the case.

We also attempted to measure the stoichiometry of Fe(II) binding to MtF by pH-stat or by fluorescence quenching but were unsuccessful. The anaerobic addition of Fe(II) to MtF at pH 7.0 resulted in no production of protons nor change in the intrinsic fluorescence of the protein, suggesting limited or weak association of Fe(II) with the apoprotein (1 μM protein, 0.1 M Mops, pH 7.0).

EPR measurements of mononuclear iron species

Low temperature electron paramagnetic resonance (EPR) measurements were undertaken to establish whether a significant amount of

mononuclear iron(III) species are formed during iron oxidation in MtF as would be expected if each of the 24 ferroxidase centers were occupied by a single Fe(III). Figure 2 shows the EPR spectra of the wild-type MtF and its variant S144A and of recombinant mouse H-chain ferritin (MoHF) with 48 or 200 Fe(II)/shell added to the protein. (Recombinant mouse H-chain ferritin (MoHF) has 93% amino acid sequence homology to human H-chain ferritin but is similar to MtF in that it has a serine residue present in position 144.) The spectrum of a 50% saturated (monoferric) human serum transferrin used as an EPR intensity standard is also shown. Double integration of the EPR spectra shows only weak $g=4.3$ signals of mononuclear $S=5/2$ Fe(III) species when compared to the control sample of transferrin, indicating that none of the
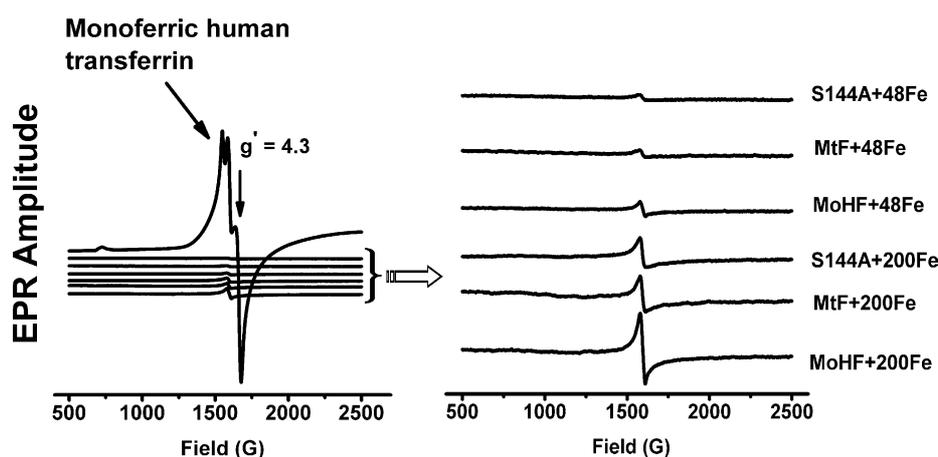
Figure 2. EPR spectra of frozen solutions of monoferric serum transferrin, S144A, MtF and MoHF. Conditions: 10.42 μM protein for 48 Fe(II)/shell, 2.5 μM protein for 200 Fe(II)/shell, 0.5 mM Fe(II), in 0.1 M Mops (pH 7.0). The transferrin sample (1 mM protein, 0.5 mM Fe) was prepared by adding a small volume of an $Fe-(NTA)_2$ solution prepared from an NTA solution and a ferric chloride hexahydrate standard solution in 3% HCl (Ricca Chemical company) to a protein sample containing 20 mM bicarbonate ($NaHCO_3$), 0.1 M Mes (pH 6.50). EPR parameters: power 20.44 mW, modulation amplitude 10 G, time constant 81.92 ms, sweep time 83.89 ms, center field 1500 G, scan range 2000 G, and microwave frequency 9.5425 GHz.

ferritin samples has significant amounts of mono-nuclear iron(III) (only 0.68 and 5.2 Fe/shell for the 48 and 200 Fe/shell additions to MtF, respectively). Therefore, the oxidation stoichiometry of 24 Fe(III)/protein noted above for MtF, S144A and for MoHF (see below) appears to be due to binding of pairs of iron atoms at only 12 of the 24 ferroxidase centers of all these proteins, a result confirmed by stopped-flow kinetics measurements demonstrating formation of a peroxodiFe(III) complex at the ferroxidase center (see below).

## Kinetics of Fe(II) oxidation measured by UV spectrophotometry

Ferroxidation and mineralization reactions in MtF, S144A, MoHF and HuHF

To further examine whether the mutation at position 144 is functionally important, we characterized the ferroxidation and mineralization reactions of MoHF for comparison with those of MtF and S144A. Accordingly, the initial rates of Fe(II) oxidation were monitored at 305 nm where μ-oxo/hydroxo Fe(III) species absorb (from the work done by Zhao et al.,[23] and references therein) following multiple eight Fe(II)/protein additions to the same protein sample. MtF, S144A and MoHF all showed a discontinuity in rate at about 24 Fe(II)/protein added (not shown), in agreement with the stoichiometry results in Figure 1, whereas HuHF, as expected, showed a discontinuity at 48 Fe(II)/protein added as reported.[25] At high iron loadings (i.e. 200 Fe/protein), variant S144A but not MtF overcomes this reduced iron binding stoichiometry as demonstrated below by the stopped-flow experiments where 24 peroxo dimers are formed in this variant, similarly to HuHF. Thus, the presence of serine at position 144 in MtF and MoHF appears to

contribute to the partial iron binding and oxidation stoichiometries observed at low iron loadings, presumably due to limited or weak iron binding under these conditions.

The initial rates of the iron mineralization reaction in MtF, S144A, MoHF and HuHF were also compared following the additions of 48, 300 or 1000 Fe(II)/shell under various conditions of pH, ionic strength, and protein concentration. As shown in Figure 3(a), at 1000 Fe(II)/protein, HuHF and MoHF display hyperbolic kinetics characteristic of a protein catalyzed reaction whereas MtF and S144A exhibit sigmoidal kinetics typical of an autocatalytic mineral surface reaction. MtF has by far the slowest iron oxidation rates of all the proteins under all conditions (Figure 3(b)). Mutation of Ser144 to Ala in variant S144A enhances the rate by ∼30–100% compared to MtF. However, MoHF having Ser144 in place of Ala exhibits kinetics typically twice as fast as HuHF. Thus, the presence or absence of Ser144 in ferritin does not by itself explain the disparate kinetics observed for the different ferritins.

Accordingly, site-directed mutagenesis was further employed to search for the origin of the markedly slower kinetics of iron oxidation in MtF. Since the ferroxidase center residues are conserved between HuHF and MtF, we examined nearby residues that differ between the two proteins. To this end, double mutations were prepared where Ser144 and Arg60 were changed to Ala and His, and Ser144 and Thr63 to Ala and Arg, respectively, their HuHF (and MoHF) homologues. Also, because of the presence of a possible hydrogen bond between Tyr34 and Glu107 in MtF, but not in HuHF, and the presence of a bulkier serine residue in MtF, which may concurrently contribute to the slower iron oxidation rates, a third double mutation (S144A/Y34F) was prepared. In all three double variants,   S144A/R60H,   S144A/T63R,   and
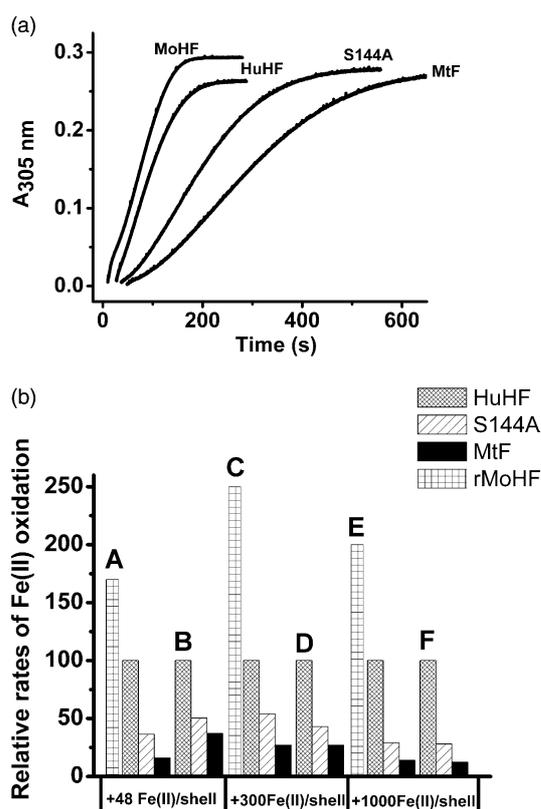
Figure 3. (a) Absorbance-time curves at 305 nm following the additions of 1000 Fe(II)/shell to MoHF, HuHF, S144A and MtF. Conditions: 0.1 μM protein, 100 μM Fe(II), 0.1 M Mops, 50 mM NaCl, pH 7.0 and 25 °C. The curves are shifted on the X-axis for clarity. (b) Relative rates of Fe(II) oxidation *versus* the amount of iron added to the protein. Conditions for: A, 0.5 μM protein, 48 Fe(II)/shell, 0.1 M Mops or Hepes, pH 7.0; B, 1 μM protein, 48 Fe(II)/shell, 70 mM Mes, 50 mM NaCl, pH 6.50; C, 0.5 μM protein, 300 Fe(II)/shell, 0.1 M Mops or Hepes, pH 7.0; D, 0.5 μM protein, 300 Fe(II)/ shell, 0.1 M Hepes, 150 mM NaCl, pH 7.0; E, 0.5 μM protein, 1000 Fe(II)/shell, 0.1 M Mops or Hepes, pH 7.0; F, 0.1 μM protein, 1000 Fe(II)/shell, 0.1 M Mops, 50 mM NaCl, pH 7.0; 25 °C.

S144A/Y34F, the kinetics were sigmoidal and the rates of iron oxidation were not significantly different from the single variant S144A of MtF, precluding the involvement of any of these additional residues in the faster iron oxidation rates observed with HuHF and MoHF (data not shown).

Regeneration of ferroxidation activity

We also examined these proteins for their abilities to regenerate ferroxidase activity. Fe(II) was added at a Fe(II)/protein ratio just enough to saturate the ferroxidase centers (i.e. 48 Fe(II)/shell for HuHF; 24 Fe(II)/shell for MtF, S144A and MoHF; 2 μM protein, 100 mM Mops, pH 7.0), followed by a similar Fe(II) addition some time later. HuHF and MoHF regenerate up to 65% of their initial

ferroxidase activities after allowing the protein samples to stand for 40 minutes, as measured by the initial rates of iron oxidation monitored at 300 nm ($0.31 \, \text{s}^{-1}$ and $0.20 \, \text{s}^{-1}$ for the first and second 48 Fe(II)/shell addition to HuHF, and $0.27 \, \text{s}^{-1}$ and $0.16 \, \text{s}^{-1}$ for the first and second 24 Fe(II)/shell addition to MoHF. S144A regenerates only about 30% of its initial ferroxidase activity after 24 hours ($0.13 \, \text{s}^{-1}$ for the first 24 Fe(II)/shell addition, and $0.037 \, \text{s}^{-1}$ for the second addition), whereas MtF does not show an initial rapid ferroxidation activity when compared to the other proteins; the initial rates of iron oxidation at 300 nm are similar for the first and second 24 Fe(II)/shell addition ($0.017 \, \text{s}^{-1}$ for the first 24 Fe(II)/shell addition and $0.014 \, \text{s}^{-1}$ for the second iron addition 24 hours later). These findings are consistent with the protein-based catalysis associated with the hyperbolic kinetics of HuHF and MoHF and with the mineral surface catalysis associated with the sigmoidal kinetics of MtF and S144A. The lack of iron turnover at the ferroxidase site of MtF is further evidenced by the failure of MtF to develop an absorbance plateau at 650 nm in stopped-flow kinetics measurements at high iron flux into the protein (data not shown). In HuHF, this absorbance plateau is attributed to iron turnover at the ferroxidase site and regeneration of ferroxidase activity.[23]
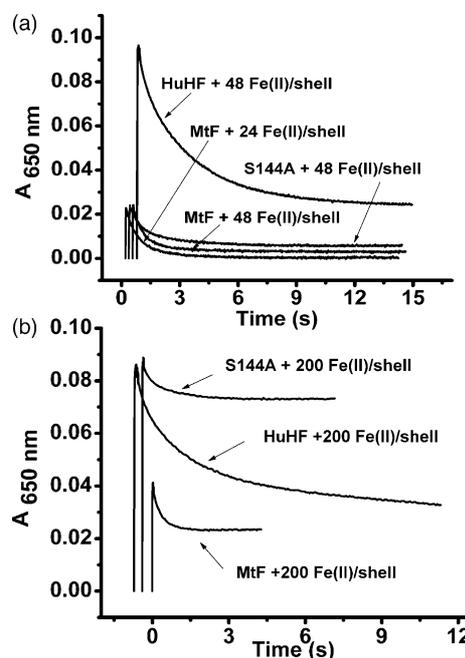
Figure 4. Stopped-flow kinetic measurements of the formation and decay of the μ-peroxodiferric intermediate in MtF, S144A and HuHF. Conditions: 4 μM protein, (a) 0.096 mM (24 Fe(II)/shell), 0.192 mM (48 Fe(II)/shell), and (b) 0.8 mM (200 Fe(II)/shell), $FeSO_4$ (pH 3.0), 50 mM Mops, pH 7.0, 21% O_2, 25 °C. The reported values are final concentrations after mixing the two reagents in the stopped-flow cell. For easy comparison, kinetic curves are offset on the time axis relative to each other. Only the early parts of the kinetics are shown in (b).

Peroxodi-iron(III) complex formation

Stopped-flow absorption spectrometry of the binding and oxidation of Fe(II) in MtF showed that a μ-peroxodi-iron(III) intermediate ($\lambda_{max} = 650$ nm) is formed at the ferroxidase center (Figure 4) as found for other ferritins.[23,26,27] The maximal concentration of the intermediate is achieved at about 50 ms in both MtF and variant S144A (Figure 4) with a formation rate constant $k_1 = 79.5(\pm 1.4)$ s^{-1} similar to that of HuHF.[8,26] (In Figure 4, the various kinetic traces have been shifted on the time axis relative to one another for better viewing). Figure 4(a) shows that the maximal 650 nm absorbances of the peroxodiFe(III) complexes in MtF and S144A are only about one-quarter that of HuHF for the 48 Fe(II)/shell addition. If we assume that the peroxo complexes of MtF and S144A have the same molar absorptivity as other ferritins ($\varepsilon = 900–1000$ M^{-1} cm^{-1}), this result implies that only about six Fe(III) peroxo dimers are formed at the ferroxidase centers of MtF and S144A compared to 24 peroxo dimers formed in HuHF under these conditions. However, at higher iron loadings (200 Fe/shell), variant S144A exhibits a similar maximal absorbance to that of HuHF (Figure 4(b)), a result indicating that iron saturation of all 24 ferroxidase centers can ultimately be obtained with this variant. Under the same conditions of 200 Fe/shell, the absorbance value for MtF reaches only half that of HuHF or S144A, an observation consistent with the formation of a maximum of 12 peroxodimers in MtF and in accord with the 24 Fe(III)/protein stoichiometry established in Figure 1. It is noteworthy that the peroxo intermediate seen in S144A is more stable than those in MtF and HuHF. In variant S144A, the intermediate lingers after a small initial rapid decay, accounting for much of the non-zero absorbance seen at the end of its kinetic trace in Figure 4(b).

Fe(II) oxidation stoichiometry in MtF

### Ferroxidation reaction with O_2 as the oxidant

The stoichiometries of iron oxidation and hydrolysis in MtF were determined to define the reaction equations for core formation. The kinetic curves for oxygen consumption and proton production are shown in Figure 5 for different iron loadings of the protein. Curves A, B, and C represent different samples to which a single addition of 48 Fe(II)/shell or two additions of 24 or 350 Fe(II)/shell were made, respectively. The similarities in the shape of the oxygen consumption and proton production curves indicate that Fe(II) oxidation and hydrolysis reactions are coupled to each other. Accordingly, when 24 Fe(II)/shell are added to apoMtF (1 μM) in the presence of 21% O_2, stoichiometric ratios of Fe(II)/O_2 = 2.1($\pm$0.1) and H$^+$/Fe(II) = 1.5($\pm$0.1) are obtained (Figure 5).

The Fe(II)/O_2 stoichiometry of ~2/1 obtained from oximetry measurements suggests that H_2O_2 is
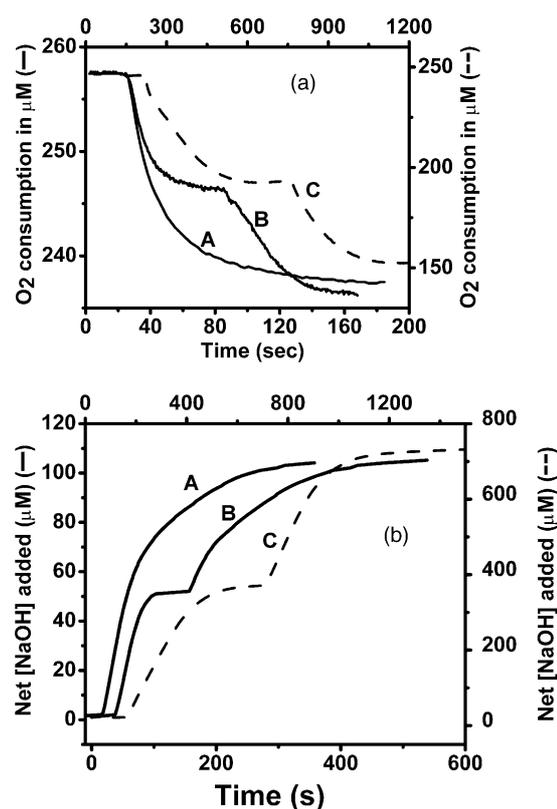
Figure 5. (a) Oxygen consumption curves and (b) net sodium hydroxide added as a function of time for: A, 24, B, 48, and C, 350 Fe(II)/MtF. Conditions: 1 μM protein for: A and B 0.5 μM protein for C in 0.3 mM Mes, 100 mM NaCl, pH 6.50.

a product of iron oxidation in accord with known ferroxidation reactions of other ferritins.[23,25,28] This expectation was confirmed using the Amplex Red reagent/horseradish peroxidase assay for H_2O_2. Hydrogen peroxide was detected as a product for both the ferroxidation (24 Fe(II)/protein, pH 7.4) and mineralization (300 Fe(II)/protein, pH 7.4) reactions in MtF (data not shown) as previously seen with HuHF.[23,29] Moreover, the addition of catalase at the end of the ferroxidation reaction following the addition of 24 or 48 Fe(II)/shell to apoMtF showed production of O_2, as measured by oximetry, and seen with HuHF,[29] a result further indicating the presence of free H_2O_2 in solution. Thus, we write the net ferroxidation reaction at the 12 active ferroxidase centers of MtF as follows:

$$2Fe^{2+} + P^Z + O_2 + 3H_2O \rightarrow (Fe_2 - O_2(OH)$$

$$- P)^{Z+1} + 3H^+ + H_2O_2 \qquad (1)$$
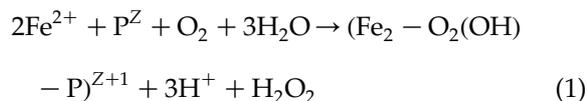
where $(Fe_2–O_2(OH)–P)^{Z+1}$ represents a μ-oxo-(hydroxo)-bridged di-iron species that has a molar absorptivity of 3400($\pm$200) M^{-1} cm^{-1} per iron at 305 nm, a value similar to that observed with other ferritins.[6,13,23,25,28–31]

EPR spin trapping experiments using the

trapping reagent (5-ethoxycarbonyl-5-methyl-1-pyrroline-*N*-oxide (EMPO) failed to trap super-oxide radical, suggesting that O_2^- is not an intermediate formed during H_2O_2 production in ferritin. Previous studies with horse spleen ferritin attempted to trap this radical but were also unsuccessful.[32]

### Mineralization reaction with O_2 as the oxidant

The stoichiometries of Fe(II) oxidation by O_2 and the number of H^+ produced were also determined when iron was added beyond a ratio of 24 Fe(II)/shell, the amount required to saturate the ferroxidase centers in MtF. When a second 24 Fe(II)/shell was added to a protein sample already containing 24 Fe(III)/shell at pH 7.0, the ratio of Fe(II)/O_2 increased from 2.0 to 2.4($\pm$0.2) and that of H^+/Fe(II) from 1.5 to 2.0($\pm$0.1). Similarly, when 350 Fe(II)/shell were added to apoMtF in one addition, stoichiometric ratios of Fe(II)/O_2 = 3.3 ($\pm$0.20), and H^+/Fe(II) = 1.9($\pm$0.1) were obtained. When a second 350 Fe(II)/shell was added to the same protein sample, the ratio of H^+/Fe(II) remained constant ($\sim$2.0($\pm$0.1)) whereas the ratio of Fe(II)/O_2 increased to 4.0($\pm$0.1). The stoichiometric changes from Fe(II)/O_2 $\sim$2 to $\sim$4 and from H^+/Fe(II) $\sim$1.5 to $\sim$2.0 as more iron is added to the protein indicate a change in the mechanism of Fe(II) oxidation from that of ferroxidation to mineralization. From the measured stoichiometries, the net mineralization reaction can be written as:

$$4Fe^{2+} + O_2 + 6H_2O \rightarrow 4FeOOH_{(core)} + 8H^+ \quad (2)$$
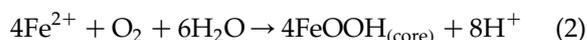
The oxygen consumption curves and the initial rates of oxygen uptake for both MtF and HuHF (Figure 6) indicate that iron oxidation in MtF is slower than that in HuHF for multiple additions of 24 or 48 Fe(II)/shell to the same protein sample. The data show that the oxygen consumption rates are comparable for the first 24 Fe(II)/shell added to both proteins (Figure 6(a), inset) but are twice as fast in HuHF than in MtF for a single addition of 48 Fe(II)/shell (Figure 6(b), inset), suggesting that half of the ferroxidase centers in MtF are functional, and consistent with the binding of only 24 Fe(III) to the protein. In addition, MtF is not able to oxidize large amounts of iron as fast as HuHF (Figure 3).

Fe(II) oxidation by H_2O_2 in MtF

It has been shown that iron oxidation in HuHF occurs by at least three different pathways, one of which involves the oxidation of two Fe(II) per H_2O_2 through a "detoxification" reaction.[23] A two Fe(II)/H_2O_2 reaction stoichiometry suggests that the production of hydroxyl radicals through Fenton chemistry, which has a stoichiometry of one Fe(II)/H_2O_2, would be minimal, an expectation borne out by the EPR spin trapping experiments with HuHF.[23] To determine whether MtF facilitates a similar detoxification reaction, spectrophotometric
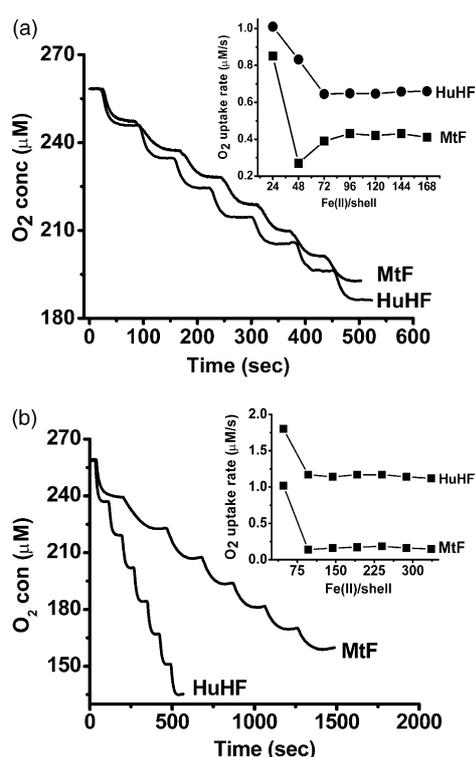
Figure 6. Oxygen consumption curves *versus* time for Fe(II) oxidation in MtF and HuHF after seven consecutive additions of (a) 24 Fe(II)/protein or (b) of 48 Fe(II)/protein. Insets: initial rates of oxygen uptake *versus* the ratio of Fe(II)/protein. Conditions: (a) 1 µM protein, 24 µM Fe(II) per protein and per addition, 0.1 M Mops, 50 mM NaCl, pH 7.0, 25 °C; (b) 1 µM protein, 48 µM Fe(II) per protein and per addition, 0.3 mM Mes, 100 mM NaCl, pH 6.50, 25 °C.

titrations were carried out anaerobically with MtF samples having 24 or 500 Fe(II)/shell. Addition of Fe(II) to apoMtF anaerobically produced no perceptible changes in the UV–visible spectrum, but upon titration with H_2O_2, a shoulder with a maximum
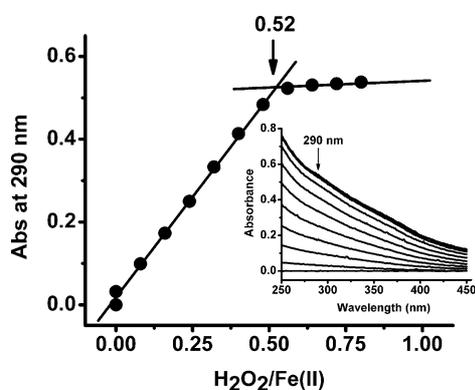
Figure 7. Spectrophotometric titration curve of iron oxidation in MtF by H_2O_2 for 500 Fe(II)/shell. Inset: absorption spectra. Conditions: 0.2 µM protein, 0.1 M Mops, pH 7.0, 500 Fe(II)/shell, under argon atmosphere. H_2O_2 was added anaerobically in a ratio of 0.08 H_2O_2/Fe(II)/addition.

absorbance near 290 nm emerged (Figure 7). A stoichiometry of ~ 0.5 H_2O_2/Fe(II) was obtained for the 500 Fe(II)/protein sample (Figure 7), indicating that one H_2O_2 oxidizes two Fe(II) as found for HuHF.[23] A somewhat higher ratio of 0.58–0.65 H_2O_2/Fe(II) was obtained when only 24–48 Fe(II)/shell were added to the protein sample (data not shown). Although the observed Fe(II)/H_2O_2 stoichiometry of $\sim 2/1$ led us to expect minimal HO$^\cdot$ radical production in MtF, spin trapping experiments discussed below revealed that this is not the case.

EPR spin trapping of hydroxyl radicals

Figure 8(a) shows the EPR spectra obtained for the anaerobic additions of 24 and 500 Fe(II)/shell to MtF in the presence of the spin trap EMPO followed by H_2O_2 titration at 0.1 H_2O_2/Fe(II) until a ratio of 1.2 H_2O_2/Fe(II) was reached. EPR spectra of the HO$^\cdot$ radical EMPO adduct were obtained in both instances (spectra B and C) with intensities comparable to the control in the absence of MtF (spectrum A). Thus, MtF lacks the 2Fe(II)+H_2O_2 detoxification reaction seen with HuHF[23] even though MtF exhibits a reaction stoichiometry of ~ 2 Fe(II)/H_2O_2. A similar result was recently reported for egg albumin and suggested to arise from a two-step oxidation mechanism whereby the one electron oxidation of Fe(II) with H_2O_2 produced hydroxyl radical that reacts with a second Fe(II) to give a net stoichiometry of two Fe(II)/H_2O_2.[33] In MtF, Fe(II) appears to undergo oxidation by H_2O_2 *via* two one-electron steps rather than the single pairwise two-electron process seen in HuHF.[23]

The production of hydroxyl radicals during the aerobic oxidation of Fe(II) in MtF by O_2 under low and high iron loadings to the protein was also investigated. Figure 8(b) shows that little HO$^\cdot$ radical is detected upon the aerobic addition of 48 or 350 Fe(II) to apoMtF and virtually none when 800 Fe(II) are added. This latter result is consistent with the stoichiometry of four Fe(II)/O_2 noted above for high iron loading of the protein and the complete reduction of O_2 to H_2O.

Discussion

Heme and iron–sulfur cluster syntheses are two important aspects of cellular iron metabolism. Both synthetic pathways require iron import into the mitochondria, but little is known about iron trafficking in this organelle. The major challenge for living cells is to maintain the mitochondrial iron pool in a soluble, bio-available, non-toxic form; several mitochondrial proteins have been identified and implicated in mitochondrial iron transport.[15–20] More recently, it has been shown that the mitochondrial protein frataxin specifically binds Fe^{2+}, preventing it from participation in harmful free radical reactions while providing an efficient source for iron–sulfur cluster assembly and heme

(a) - H_2O_2 oxidant
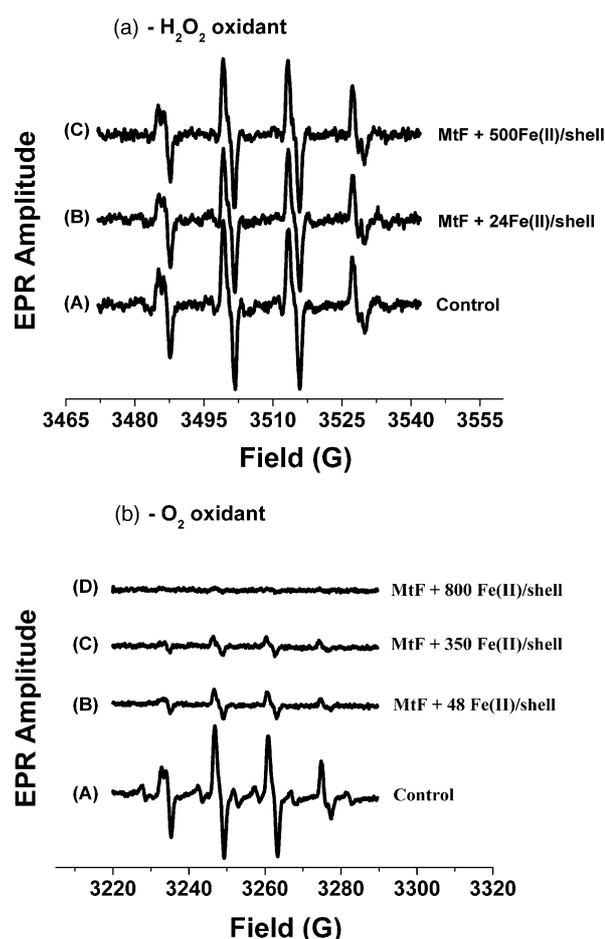
Figure 8. X-band EPR signal of the EMPO-OH adduct in the presence and absence of MtF, 0.1 M Mops (pH 7.0). In (a): A, anaerobic addition sequence of (EMPO+48 μM Fe(II)+H_2O_2) to buffer alone; B and C, anaerobic addition sequence of (EMPO+24 and 500 Fe(II)/shell+H_2O_2) to MtF (2 and 0.096 μM), respectively. In (b): A, aerobic addition sequence of EMPO+96 μM Fe(II)+H_2O_2 to buffer alone; B, C and D, aerobic addition of (EMPO + 48, 350, and 800 Fe(II)/shell) to MtF (2, 0.27, and 0.12 μM), respectively. The EMPO concentration was 25 mM and H_2O_2 was titrated in increments of 0.1 H_2O_2/Fe(II) until a ratio of 1.0–1.2 H_2O_2/Fe(II) was reached. The time interval between H_2O_2 additions was typically 20–30 seconds and the EPR measurements were done within five minutes of the last reagent or addition. Spectrometer parameters were: microwave power 5.0 mW, modulation amplitude 0.5 G, time constant 163.8 ms, sweep time 83.89 ms, signal averaged four times, room temperature. The spectra in (b) were recorded on a laboratory-assembled EPR spectrometer (Bruker ER 041 XK-H) X-band microwave bridge operating at 9.24 GHz with 100 kHz field modulation. Conditions: same as above except time constant 0.3, and scan rate 7.14 G s^{-1}.

biosynthesis.[33–36] Another important discovery is the presence of mitochondrial ferritin,[21] which is specifically targeted to the mitochondria and processed into a functional 24 subunit homopolymer protein capable of incorporating large amounts of iron similar to other ferritins.[22] Our data demonstrate for the first time that MtF has

ferroxidase activity, albeit significantly lower than normal H-chain cytosolic ferritin, and that the iron chemistry of MtF is unique in several aspects.

HuHF and MtF oxidize and deposit iron in some different ways despite the similarities of their ferroxidase centers, i.e. conserved residues and formation of μ-peroxodiFe(III) intermediates. HuHF initially oxidizes 48 Fe(II)/shell and regenerates its ferroxidase activity whereas MtF can process only 24 Fe(II)/shell, at a reduced rate, and does not regenerate ferroxidase activity. The μ-oxo(hydroxo) di-iron complex formed at the ferroxidase center of MtF (equation (1)) is also different from that formed in HuHF,[25] since the number of protons produced during iron oxidation is different, three H^+ *versus* two H^+ per two Fe(II) oxidized (equation (1)).[25] In addition, HuHF displays hyperbolic kinetics when large amounts of iron are presented to the protein (1000 Fe(II)/shell), characteristic of a protein-catalyzed oxidation reaction and rapid turnover of iron at the ferroxidase center,[23] whereas MtF shows sigmoidal kinetics of iron oxidation (Figure 3(a)), more characteristic of an autocatalytic mineral surface mechanism in which additional iron oxidation occurs at the surface of the developing iron core. Nevertheless, both MtF and HuHF can effectively store large amounts of iron (up to 2000 Fe/shell), the maximum amount of iron attempted. Even hydrogen peroxide that is produced during the ferroxidation and mineralization reactions in both ferritins as shown by this work and elsewhere,[23,29] is used differently by the two proteins. HuHF effectively uses the H_2O_2 produced to oxidize additional Fe(II) pairwise, thus minimizing the production of hydroxyl radicals[23] and further contributing to building the iron core, whereas MtF does not, as shown in Figure 8(a). However, because the mineral surface reaction in MtF begins to occur at an earlier stage, after only 24 Fe(II)/shell have been added to MtF compared to 48 Fe(II)/shell in HuHF,[23] MtF may largely avoid Fenton chemistry by shifting the mechanism of Fe(II) oxidation from equation (1) to (2) earlier during core formation than in HuHF and accounting for the minimal $HO^·$ radical produced with O_2 as the oxidant (Figure 8(b)). The iron oxidation stoichiometries are similar for HuHF and MtF in that a ratio of two Fe(II)/O_2 is first observed at low iron loadings ($\leq$24 Fe(II)/shell) climbing to four Fe(II)/ O_2 as more iron is added to the protein. Thus complete reduction of O_2 to H_2O ultimately occurs in both proteins (but at a lower Fe/protein ratio in MtF).

The lack of iron turnover at the ferroxidase center of MtF is also observed in the ferritins from *E. coli*, namely bacterioferritin EcBFR, and bacterial ferritin EcFtnA.[37,38] However, MtF displays much slower sigmoidal kinetics at large iron loadings of the protein ($>$300 Fe/protein) compared to the fast hyperbolic kinetics of EcBFR and EcFtnA. In the bacterial ferritins, the ferroxidase center perhaps also functions as the nucleation site for core

formation. In contrast, the negative patch of Glu residues near the ferroxidase center in MtF[24] may constitute the nucleation sites in this protein, thus accounting for its slow sigmoidal kinetics as also found for L-chain ferritin having a similar negative patch of residues.[9,23]

The crystal structure of MtF has been recently solved and is very similar to that of HuHF, as expected from the close correspondence of their amino acid sequences.[24] Interestingly, site A (consisting of residues Glu27, Glu62, and His65) of the ferroxidase center of MtF was found always occupied by a metal ion whereas the occupancy of site B (consisting of residues Glu62, and Glu107) was variable and depended on the metal ion used (40% for Mn^{2+}, 100% for Zn^{2+}, and no Mg^{2+} were found at site B). More importantly, variant S144A showed a higher B-site occupancy with all metal ions, an observation consistent with its increased ferroxidase activity observed here. Indeed, the crystal structure of MtF shows that the side-chain of serine 144 protrudes toward a channel that connects to the ferroxidase center, thus making the pathway of iron to this site narrower than when alanine is present as in HuHF. Such a disposition of residues creates steric hindrance that may prevent the easy access of iron or other metal ions to the ferroxidase centers and account for the partial iron oxidation stoichiometry of 24 Fe/protein observed here with MtF and MoHF. When serine 144 was mutated to alanine, faster kinetics (up to 100% faster in S144A than MtF, Figure 3) were observed. However, the ferroxidase activity of variant S144A was still lower than that of HuHF, suggesting that other residues or factors are involved. The three double mutants S144A/R60H, S144A/T63R and S144A/Y34F showed similar ferroxidation activities to that of the single variant S144A, precluding residues 34, 60 and 63 as important in catalysis.

Because fewer ferroxidase centers in MtF appear to be involved in peroxo complex formation (i.e. a maximum of ∼12) as shown in Figure 4, the slower rate of iron oxidation in MtF compared to HuHF is probably due, in part, to its lower number of functional ferroxidase centers as well as the lack of iron turnover at these centers. The lack of iron turnover means that a mineral surface mechanism, which is inherently slower in oxidizing iron than the protein-catalyzed mechanism, comes into play. Mouse H-chain ferritin (MoHF) exhibits a binding stoichiometry of only 24 Fe/protein as in MtF, has Ser144 in place of Ala144 and displays fast hyperbolic oxidation kinetics (Figure 3), presumably in part because of turnover of iron at its ferroxidase centers.

The first iron oxidation product in most ferritins is the μ-peroxodiFe(III) intermediate, which is formed within the first 50 ms of the reaction[8,26,27,39] (Figure 4) and has an estimated molar absorptivity of about 1000 M^{-1} cm^{-1} at 650 nm on a per Fe(III) dimer basis.[26,27] The rates of formation and decay of this intermediate in MtF are close to those reported for HuHF and other ferritins.[26,27] In HuHF, all 24

ferroxidase centers are functional and able to bind, oxidize, and turnover iron. The lack of iron binding at all 24 ferroxidase centers of MtF and MoHF may reflect some negative cooperativity between centers upon iron binding, an effect mediated in part by Ser144 since, in variant S144A, all 24 ferroxidase centers form peroxo complexes at sufficiently high iron loading of the protein (Figure 4(b)). Alternatively, the binding and oxidation of iron at 12 of the 24 ferroxidase centers may induce asymmetry in the protein through an allosteric mechanism and render the remaining 12 ferroxidase centers inactive.

The X-ray structure determination of MtF located a new metal ion binding site (Q58, H57, and E61) on the cavity surface near the ferroxidase center and not found in HuHF.[24] This site has been proposed to play a role in iron transfer from the ferroxidase center to the cavity where iron core nucleation would take place.[24] If this hypothesis were true, the ferroxidase activity of MtF would be regenerated upon the addition of more iron, since this site would facilitate the clearance of iron from the ferroxidase centers. However, our data demonstrate that the ferroxidase activity of MtF is not regenerated, even after allowing the protein to stand for two days, an observation that argues against this hypothesis. A recent investigation of the role of the putative nucleation site residues in HuHF revealed that this site is not required for mineralization of the iron core as previously thought.[26] Therefore, one attractive possibility is that the additional residues in HuHF and MtF in some way serve to retain iron longer at the ferroxidase center, thus conferring a physiological advantage by keeping iron readily accessible for use by the cell.[26,37]

Whether MtF is an essential component of the complex machinery involved in the syntheses of heme or iron–sulfur clusters remains to be determined. There is evidence that the mitochondrial protein frataxin is an iron donor for [2Fe–2S] clusters and also a mediator of iron transfer to ferrochelatase in the final step of heme biosynthesis.[34,35,40,41] Also, frataxin has been shown to reduce the level of oxidant-induced inactivation of aconitase, to protect the mitochondria from iron-induced oxidative damage, and to attenuate HO$^{\cdot}$ radical production.[33,36] A more recent study showed that the expression of human mitochondrial ferritin in frataxin-deficient yeast cells rescued respiratory functions, prevented iron accumulation in the mitochondria, and protected the activity of iron–sulfur enzymes.[42] In this context, it appears that both MtF and frataxin are mutually involved in alleviating the oxidative stress caused by excess free iron in the mitochondria and that MtF may have iron–chaperone properties, as has been suggested for frataxin.[36,41–43]

Finally, it is constructive to consider possible roles for mitochondrial ferritin in mitochondrial iron homeostasis as they relate to the present results and the current literature. First, it is pertinent that MtF is expressed in very small amounts in most normal cells but overexpressed in erythroblasts with defective heme synthesis.[22] Under pathological conditions and in the presence of excess iron, MtF has the ability to sequester large amounts of iron and act as an iron storage protein similar to cytosolic ferritins.[21,22] This proposal is supported by the discovery that most of the iron in sideroblastic anemia is found in MtF, which has been suggested to be a specific marker for this disease.[21,44] Because the mitochondria are constantly exposed to high trafficking of iron for biosynthetic pathways, it is reasonable to suggest that MtF has an iron storage function similar to that of the L-chain-rich ferritins in iron storage organs such as liver and spleen.[5] This proposal is in keeping with our kinetic studies showing that both MtF (Figure 3(a)) and L-chain[23] have similar relatively slow sigmoidal kinetics of iron oxidation. It is also noteworthy that MtF, like L-chain ferritin, has multiple nucleation sites on the cavity surface[24] that could favor mineralization of the iron core. In addition, MtF, like HuHF, has a functional ferroxidase center capable of rapidly oxidizing iron, albeit only 24 Fe/protein, but nevertheless sufficient to initiate mineralization at an early stage of iron deposition. Furthermore, cytosolic ferritin functions in an environment different from the mitochondrial environment. Thus, a ferritin working inside mitochondria may not need highly efficient ferroxidase activity as cytosolic ferritin does. The transient transfectant MtF in HeLa cells takes up iron when targeted to the mitochondria but not when present in the cytosol.[22] Thus, the mitochondrial environment appears to be more favorable than the cytosolic environment to iron incorporation in MtF.

One hypothesis is that MtF within the mitochondria may have evolved to possess the functional properties of both H and L-subunits within a single homopolymer protein. One obvious function of MtF is to store iron so that it does not participate in the production of reactive oxygen species and at the same time protect the cell from any free iron that has escaped during its transfer to other molecules, particularly during the synthesis of heme and iron–sulfur clusters. However, unexpectedly, the present work indicates that MtF does not facilitate the $2Fe(II) + H_2O_2$ detoxification reaction (Figure 8(a)) whereas several other iron processing proteins such as Dps, HuHF, *E. coli* bacterioferritin (EcBFR), and frataxin do.[13,23,31,33] Nevertheless, MtF can efficiently store iron oxidatively with O_2 as the oxidant, producing minimal hydroxyl radical as demonstrated by the EPR spin trapping measurements (Figure 8(b)).

Materials and Methods

Preparation and purification of MtF and HuHF were performed as described.[21,45] Variants S144A, S144A/R60H, S144A/T63R and S144A/Y34F of MtF were produced by oligonucleotide-directed mutagenesis of the plasmid pET-HuMtF[24] following the manufacturers' procedure (QuikChange Site Direct Mutagenesis Kit,

Stratagene). The recombinant proteins were subjected to two anaerobic reductions using 55 mM and 5 mM sodium dithionite in 50 mM Mes (2-(*N*-morpholino) ethanesulfonic acid), (pH 6.0) for three days each followed by two days of anaerobic dialysis against 1 mM 2,2′-bipyridyl and 50 mM Mes (pH 6.0).[23] The resulting solution was dialyzed against the working buffer used in the experiments. The apoprotein concentrations were determined spectrophotometrically at 280 nm using a molar absorptivity of $23,000 \, M^{-1} \, cm^{-1}$ for HuHF[23] and $17,000 \, M^{-1} \, cm^{-1}$ for MtF (the original MtF concentration being determined by the Advanced Protein Assay† using BSA as a standard). The lower molar absorptivity of MtF is consistent with its fewer aromatic residues compared to HuHF. The concentrations of freshly prepared hydrogen peroxide solutions were assayed by electrode oximetry from the amount of O_2 produced upon addition of catalase (EC 1.11.1.6, 65,000 units/mg, Roche Molecular Biochemicals) or from its absorbance at 240 nm ($\varepsilon = 43.6 \, M^{-1} \, cm^{-1}$). Fe(II) stock solutions were freshly prepared before each experiment in dilute HCl solution at pH 3.0. All chemicals employed were reagent grade and used without further purification. Mops and Hepes buffers were purchased from Research Organics (Cleveland, OH), $FeSO_4 \cdot 7H_2O$ from J. T. Baker (Phillipsburg, NJ), sodium dithionite, $Na_2S_2O_4$, and 2,2′-bipyridyl from Sigma-Aldrich Corporate (St Louis, MO).

The electrode oximetry/pH-stat apparatus, procedures, and standardization reactions have been described in detail elsewhere.[25] Background compensations for the free acid in the ferrous sulfate stock solutions were made in all H^+ ion count determinations.

Conventional UV–visible spectroscopy was performed on a Varian Cary 50 spectrophotometer. Fluorescence experiments were performed at room temperature on a Varian Cary Eclipse fluorimeter using an excitation wavelength of 280 nm and emission and excitation bandwidths of 5 nm. The EPR measurements were done on a Bruker EleXsys E-500 EPR spectrometer or with a laboratory-assembled spectrometer described elsewhere.[46] Spectrophotometric data were analyzed with Origin 7.0 software (Microcal Inc.). Experiments involving the oxidation of Fe(II) by H_2O_2 under anaerobic conditions were conducted with thoroughly deoxygenated solutions using high-purity grade argon gas (99.995%, <5 ppm O_2).

Stopped-flow absorbance measurements were conducted with a pneumatic drive Hi-Tech SFA-20M stopped-flow accessory on a J&M GmbH Tidas diode array spectrophotometer. The 650 nm absorbance of the peroxodi-iron(III) complex formed after mixing the apoprotein with Fe(II) in the presence of oxygen was monitored every 2.5 ms following the first 8 ms of reaction (the sum of which is the approximate dead time of the stopped-flow/diode array apparatus).

Acknowledgements

References

1. Andrews, S. C. (1998). Iron storage in bacteria. *Advan. Microb. Physiol.* **40**, 281–351.
2. Theil, E. C. (2001). Ferritin. In *Handbook of Metalloproteins* (Messerschmidt, A., Huber, R., Poulos, T. & Wieghardt, K., eds), pp. 771–781, John Wiley and Sons, Chichester.
3. Christen, Y. (2000). Oxidative stress and Alzheimer disease. *Am. J. Clin. Nutr.* **71**, 621S–629S.
4. Crichton, R. R. & Ward, R. J. (1995). Iron species in iron homeostasis and toxicity. *Analyst*, **120**, 693–697.
5. Harrison, P. M. & Arosio, P. (1996). Ferritins: molecular properties, iron storage function and cellular regulation. *Biochim. Biophys. Acta*, **1275**, 161–203.
6. Chasteen, N. D. & Harrison, P. M. (1999). Mineralization in ferritin: an efficient means of iron storage. *J. Struct. Biol.* **126**, 182–194.
7. Lawson, D. M., Artymiuk, P. J., Yewdall, S. J., Smith, J. M. A., Livingstone, J. C., Treffry, A. *et al.* (1991). Solving the structure of human H ferritin by genetically engineering intermolecular crystal contacts. *Nature*, **349**, 541–544.
8. Treffry, A., Zhao, Z., Quail, M. A., Guest, J. R. & Harrison, P. M. (1995). Iron II oxidation by H-chain ferritin: evidence from site-directed mutagenesis that a transient blue species is formed at the dinuclear iron center. *Biochemistry*, **34**, 15204–15213.
9. Levi, S., Santambrogio, P., Cozzi, A., Rovida, E., Corsi, B., Tamborini, E. *et al.* (1994). The role of the L-chain in ferritin iron incorporation. Studies of homo- and heteropolymers. *J. Mol. Biol.* **238**, 649–654.
10. Santambrogio, P., Levi, S., Cozzi, A., Rovida, E., Albertini, A. & Arosio, P. (1993). Production and characterization of recombinant heteropolymers of human ferritin H and L chains. *J. Biol. Chem.* **268**, 12744–12748.
11. Grant, R. A., Filman, D. J., Finkel, S. E., Kolter, R. & Hogle, J. M. (1998). The crystal structure of Dps, a ferritin homolog that binds and protects DNA. *Nature Struct. Biol.* **5**, 294–303.
12. Ilari, A., Stefanini, S., Chiancone, E. & Tsermoglou, D. (2000). The dodecameric ferritin from *Listeria innocua* contains a novel intersubunit iron-binding site. *Nature Struct. Biol.* **7**, 38–43.
13. Zhao, G., Ceci, P., Ilari, A., Giangiacomo, L., Laue, T. M., Chiancone, E. & Chasteen, N. D. (2002). Iron and hydrogen peroxide detoxification properties of DNA-binding protein from starved cells: a ferritin-like DNA-binding protein of *Escherichia coli*. *J. Biol. Chem.* **277**, 27689–27696.
14. Nicholls, D. G. (2002). Mitochondrial function and dysfunction in the cell: its relevance to aging and aging-related disease. *Int. J. Biochem. Cell. Biol.* **34**, 1372–1381.
15. Kispal, G., Csere, P., Guiard, B. & Lill, R. (1997). The ABC transporter Atm1p is required for mitochondrial iron homeostasis. *FEBS Letters*, **418**, 346–350.
16. Knight, S. A. B., Sepuri, N. B. V., Pain, D. & Dancis, A. (1998). Mt-Hsp70 homolog, Ssc2p, required for maturation of yeast frataxin and mitochondrial iron homeostasis. *J. Biol. Chem.* **273**, 18389–18393.

† http://cytoskeleton.com

17. Lange, H., Kispal, G. & Lill, R. (1999). Mechanism of iron transport to the site of heme synthesis inside yeast mitochondria. *J. Biol. Chem.* **274**, 18989–18996.

18. Gibson, T. J., Koonin, E. V., Musco, G., Pastore, A. & Bork, P. (1996). Friedreich's ataxia protein: phylogenetic evidence for mitochondrial dysfunction. *Trends Neurosci.* **19**, 465–468.

19. Cavadini, P., Gellera, C., Patel, P. I. & Isaya, G. (2000). Human frataxin maintains mitochondrial iron homeostasis in *Saccharomyces cerevisiae*. *Hum. Mol. Genet.* **9**, 2523–2530.

20. Pandolfo, M. (2002). Iron metabolism and mitochondrial abnormalities in Friedreich ataxia. *Blood Cells Mol. Dis.* **29**, 536–547.

21. Levi, S., Corsi, B., Bosisio, M., Invernizzi, R., Volz, A., Sanford, D. *et al.* (2001). A human mitochondrial ferritin encoded by an intronless gene. *J. Biol. Chem.* **270**, 24437–24440.

22. Corsi, B., Cozzi, A., Arosio, P., Drysdale, J., Santambrogio, P., Campanella, A. *et al.* (2002). Human mitochondrial ferritin expressed in HeLa cells incorporates iron and affects cellular iron metabolism. *J. Biol. Chem.* **277**, 22430–22437.

23. Zhao, G., Bou-Abdallah, F., Arosio, P., Levi, S., Janus-Chandler, C. & Chasteen, N. D. (2003). Multiple pathways for mineral core formation in mammalian apoferritin. The role of hydrogen peroxide. *Biochemistry*, **42**, 3142–3150.

24. Langlois d'Estaintot, B., Santambrogio, P., Granier, T., Gallois, B., Chevalier, J. M., Precigoux, G. *et al.* (2004). Crystal structure and biochemical properties of the human mitochondrial ferritin and its mutant Ser144Ala. *J. Mol. Biol.* **340**, 277–293.

25. Yang, X., Chen-Barrett, Y., Arosio, P. & Chasteen, N. D. (1998). Reaction paths of iron oxidation and hydrolysis in horse spleen and recombinant human ferritins. *Biochemistry*, **37**, 9743–9750.

26. Bou-Abdallah, F., Biasiotto, G., Arosio, P. & Chasteen, N. D. (2004). The putative "nucleation site" in human H-chain ferritin is not required for mineralization of the iron core. *Biochemistry*, **43**, 4332–4337.

27. Pereira, A. S., Small, W., Krebs, C., Tavares, P., Edmondson, D. E., Theil, E. C. & Huynh, B. H. (1998). Direct spectroscopic and kinetic evidence for the involvement of a peroxodiferric intermediate during the ferroxidase reaction in fast ferritin mineralization. *Biochemistry*, **37**, 9871–9876.

28. Sun, S., Arosio, P., Levi, S. & Chasteen, N. D. (1993). Ferroxidase kinetics of human liver apoferritin, recombinant H-chain apoferritin, and site-directed mutants. *Biochemistry*, **32**, 9362–9369.

29. Zhao, G., Bou-Abdallah, F., Yang, X., Arosio, P. & Chasteen, N. D. (2001). Is hydrogen peroxide produced during iron(II) oxidation in mammalian apoferritins? *Biochemistry*, **40**, 10832–10838.

30. Bou-Abdallah, F., Arosio, P., Santambrogio, P., Yang, X., Janus-Chandler, C. & Chasteen, N. D. (2002). Ferrous ion binding to recombinant human H-chain ferritin. An isothermal titration calorimetry study. *Biochemistry*, **41**, 11184–11191.

31. Bou-Abdallah, F., Lewin, A. C., Le Brun, N. E., Moore, G. R. & Chasteen, N. D. (2002). Iron detoxification properties of *Escherichia coli* bacterioferritin. Attenuation of oxyradical chemistry. *J. Biol. Chem.* **277**, 37064–37069.

32. Xu, B. & Chasteen, N. D. (1991). Iron oxidation chemistry in ferritin. Increasing Fe/O2 stoichiometry during core formation. *J. Biol. Chem.* **266**, 19965–19970.

33. Bou-Abdallah, F., Adinolfi, S., Pastore, A., Laue, T. M. & Chasteen, N. D. (2004). Iron binding and oxidation properties of the bacterial frataxin CyaY of *Escherichia coli*. *J. Mol. Biol.* **341**, 605–615.

34. Yoon, T. & Cowan, J. A. (2003). Iron–sulfur cluster biosynthesis. Characterization of frataxin as an iron donor for assembly of [2Fe–2S] clusters in ISU-type proteins. *J. Am. Chem. Soc.* **125**, 6078–6084.

35. Yoon, T. & Cowan, J. A. (2004). Frataxin-mediated iron delivery to ferrochelatase in the final step of heme biosynthesis. *J. Biol. Chem.* **279**, 25943–25946.

36. Bulteau, A.-L., O'Neill, H. A., Kennedy, M. C., Ikeda-Saito, M., Isaya, G. & Szweda, L. I. (2004). Frataxin acts as an iron chaperone protein to modulate mitochondrial aconitase activity. *Science*, **305**, 242–245.

37. Treffry, A., Zhao, Z., Quail, M. A., Guest, J. R. & Harrison, P. M. (1998). How the presence of three iron binding sites affects the iron storage function of the ferritin (EcFtnA) of *Escherichia coli*. *FEBS Letters*, **432**, 213–218.

38. Yang, X., Le Brun, N. E., Thomson, A. J., Moore, G. R. & Chasteen, N. D. (2000). The iron oxidation and hydrolysis chemistry of *Escherichia coli* bacterioferritin. *Biochemistry*, **39**, 4915–4923.

39. Bou-Abdallah, F., Papaefthymiou, G. C., Scheswohl, D. M., Stanga, S. D., Arosio, P. & Chasteen, N.D.(-1. (2002). 2-Peroxobridged di-iron(III) dimer formation in human H-chain ferritin. *Biochem. J.* **364**, 57–63.

40. Gerber, J., Muehlenhoff, U. & Lill, R. (2003). An interaction between frataxin and Isu1/Nfs1 that is crucial for Fe/S cluster synthesis on Isu1. *EMBO Rep.* **4**, 906–911.

41. Park, S., Gakh, O., O'Neill, H. A., Mangravita, A., Nichol, H., Ferreira, J. C. & Isaya, G. (2003). Yeast frataxin sequentially chaperones and stores iron by coupling protein assembly with iron oxidation. *J. Biol. Chem.* **278**, 31340–31351.

42. Campanella, A., Isaya, G., O'Neill, H. A., Santambrogio, P., Cozzi, A., Arosio, P. & Levi, S. (2004). The expression of human mitochondrial ferritin rescues respiratory function in frataxin-deficient yeast. *Hum. Mol. Genet.* **13**, 2279–2288.

43. Isaya, G., O'Neill, H. A., Gakh, O., Park, S., Mantcheva, R. & Mooney, S. M. (2004). Functional studies of frataxin. *Acta Paediatr.* **93**, 68–73.

44. Cazzola, M., Invernizzi, R., Bergamaschi, G., Levi, S., Corsi, B., Travaglino, E. *et al.* (2003). Mitochondrial ferritin expression in erythroid cells from patients with sideroblastic anemia. *Blood*, **101**, 1996–2000.

45. Santambrogio, P., Cozzi, A., Levi, S., Rovida, E., Magni, F., Albertini, A. & Arosio, P. (2000). Functional and immunological analysis of recombinant mouse H- and L-ferritins from *Escherichia coli*. *Protein Expr. Purif.* **19**, 212–218.

46. Yang, X. & Chasteen, N. D. (1996). Molecular diffusion into horse spleen ferritin: a nitroxide radical spin probe study. *Biophys. J.* **71**, 1587–1595.

Edited by R. Huber